

## Observation of orbital order in the van der Waals material 1T-TiSe<sub>2</sub>

Yingying Peng,<sup>1,\*</sup> Xuefei Guo,<sup>2</sup> Qian Xiao,<sup>1</sup> Qizhi Li,<sup>1</sup> Jörg Strempler<sup>3</sup>, Yongseong Choi<sup>3</sup>, Dong Yan,<sup>4,5</sup> Huixia Luo,<sup>4</sup> Yuqing Huang,<sup>1</sup> Shuang Jia,<sup>1</sup> Oleg Janson<sup>6</sup>, Peter Abbamonte,<sup>2</sup> Jeroen van den Brink,<sup>6,7,8</sup> and Jasper van Wezel<sup>8,†</sup>

<sup>1</sup>International Center for Quantum Materials, School of Physics, Peking University, Beijing 100871, China

<sup>2</sup>Department of Physics and Materials Research Laboratory, University of Illinois, Urbana, Illinois 61801, USA

<sup>3</sup>Advanced Photon Source, Argonne National Laboratory, Argonne, Illinois 60439, USA

<sup>4</sup>School of Materials Science and Engineering, State Key Laboratory of Optoelectronic Materials and Technologies, Sun Yat-Sen University, Guangzhou 510275, China

<sup>5</sup>Key Laboratory of Functional Molecular Solids, Ministry of Education, College of Chemistry and Materials Science, Anhui Normal University, Wuhu 241002, China

<sup>6</sup>Institute for Theoretical Solid State Physics, IFW Dresden, Helmholtzstrasse 20, 01069 Dresden, Germany

<sup>7</sup>Würzburg-Dresden Cluster of Excellence *ct.qmat*, TU Dresden, 01069 Dresden, Germany

<sup>8</sup>Institute for Theoretical Physics Amsterdam, University of Amsterdam, Science Park 904, 1098 XH Amsterdam, The Netherlands



(Received 2 March 2022; accepted 27 June 2022; published 18 July 2022)

Besides magnetic and charge order, regular arrangements of orbital occupation constitute a fundamental order parameter of condensed matter physics. Even though orbital order is difficult to identify directly in experiments, its presence was firmly established in a number of strongly correlated, three-dimensional Mott insulators. Here, reporting resonant x-ray-scattering experiments on the layered van der Waals compound 1T-TiSe<sub>2</sub>, we establish that the known charge density wave in this weakly correlated, quasi-two-dimensional material corresponds to an orbital ordered phase. Our experimental scattering results are consistent with first-principles calculations that bring to the fore a generic mechanism of close interplay between charge redistribution, lattice displacements, and orbital order. It demonstrates the essential role that orbital degrees of freedom play in TiSe<sub>2</sub>, and their importance throughout the family of correlated van der Waals materials.

DOI: [10.1103/PhysRevResearch.4.033053](https://doi.org/10.1103/PhysRevResearch.4.033053)

### I. INTRODUCTION

Quasi-two-dimensional van der Waals (VdW) materials are layered solids with strong in-plane covalent bonding and weak interlayer VdW interactions, that have become a focal area for materials research in recent years [1–10]. The success of graphene—which stems from the paradigmatic VdW material graphite—in particular triggered a search for similar VdW materials that can be exfoliated to the monolayer limit, but which harbor physical properties beyond those of graphene [11,12]. Magnetic ordering for example, has been observed in the VdW materials CrX<sub>3</sub> ( $X = \text{Cl, Br, I}$ ) [2–4], Cr<sub>2</sub>Ge<sub>2</sub>Te<sub>6</sub> [5], and NiPS<sub>3</sub> [6].

The family of transition-metal dichalcogenides (TMDCs) is a particularly promising group of VdW materials, that can be straightforwardly prepared in atomically thin configurations and device settings [12]. They typically harbor multiple competing and coexisting phases of matter, which

allow a fine tuning of the phase diagram and material properties in response to external stimuli like pressure, intercalation, or gating [13–15]. At the same time, however, uncertainty and controversy surround the ground state order in several TMDCs. This is especially striking in the case of 1T-TiSe<sub>2</sub>, for which charge density wave (CDW) order was discovered below  $T_{\text{CDW}} \simeq 200$  K decades ago [16]. Debates about its nature and driving mechanism, however, are only recently converging towards a combination of exciton formation and lattice effects stabilizing a condensate of particle-hole pairs [17–25], while debate about its potential chirality continues until the present day [26–31]. Within this context, we establish here that additionally the electronic ground state in 1T-TiSe<sub>2</sub> has a nontrivial orbital structure.

At the center of the rich phase diagram and versatility of TMDC materials, but also of their controversies, lie the transition-metal  $d$  orbitals. Their spatially compact but not fully localized electronic wave functions allow small changes in the occupation of these orbitals to have a strong effect on the atomic displacement of neighboring chalcogens, on the distribution of electron charges between atoms, on the coupling of electronic excitations to phonons, and even on the structuring of spins [26,32–35]. Unveiling any patterns of orbital occupation therefore offers a novel crucial element for understanding the nature and emergence of order in transition-metal dichalcogenides.

\*yingying.peng@pku.edu.cn

†vanwezel@uva.nl

Published by the American Physical Society under the terms of the [Creative Commons Attribution 4.0 International](https://creativecommons.org/licenses/by/4.0/) license. Further distribution of this work must maintain attribution to the author(s) and the published article's title, journal citation, and DOI.

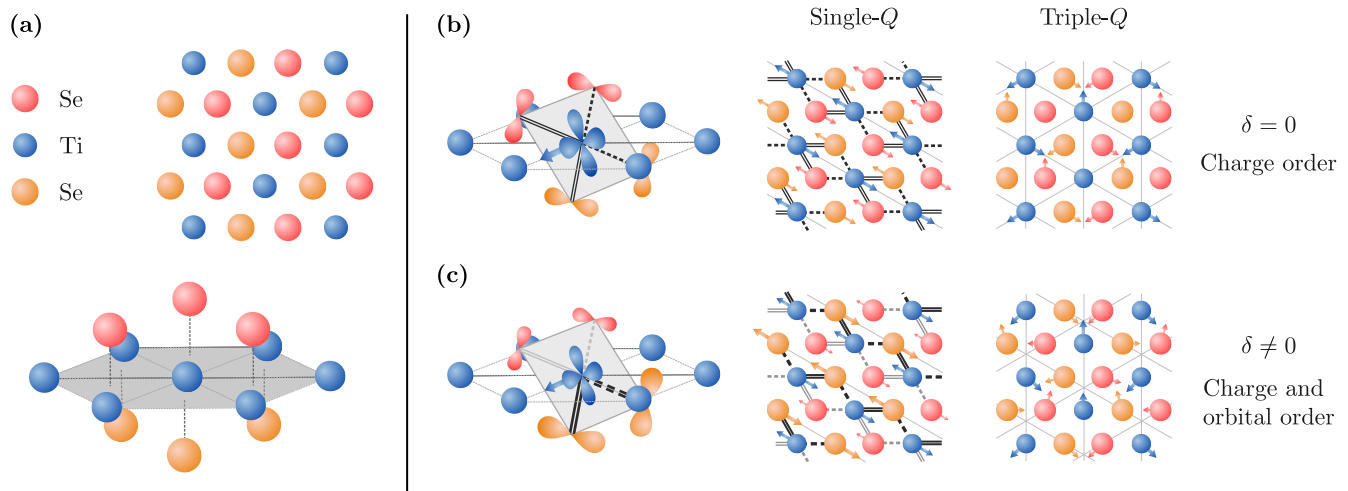


FIG. 1. Charge and orbital order in  $1T$ -TiSe<sub>2</sub>. (a) Top-view and three-dimensional sketch of the atomic structure within a single layer of  $1T$ -TiSe<sub>2</sub> in the high-temperature phase (space group 164,  $P\bar{3}m1$ ). (b) The charge ordered phase without relative phase shifts (space group 165,  $P\bar{3}c1$ ). The local charge transfer process for one of the CDW components and all orbitals involved in it are shown in the three-dimensional structure, followed by a top view of the displacements and charge transfers in a single CDW component, and finally the full displacement pattern in the triple- $Q$  structure actually realized in TiSe<sub>2</sub>. Extrema of the CDW are indicated by faint gray lines and atomic displacements by arrows (exaggerated for clarity). Double lines indicate an electronic bonding state between neighboring atoms, while dashed lines depict an electronic antibonding state. (c) The orbital ordered state proposed in Ref. [26], resulting from relative phase shifts  $\delta$  between CDW components (space group 5,  $C2$ ). The sliding of a single component causes the charge transfer processes to be centered on either the upper or lower Se layer. As a result, the atomic displacements and orbital occupations associated with different CDW components differ in amplitude. This results in a slight alteration to the distortion pattern, as well as an ordered redistribution of electronic charge among the titanium  $t_{2g}$  orbitals.

That the orbital degree of freedom of electrons in a solid material can be ordered in the same fashion as the electron's charge or spin was pointed out in the 1970s [36,37]. Even if electrons in solids form bands and delocalize from the nuclei, in Mott insulators they retain their three fundamental quantum numbers: spin, charge, and orbital. This observation sparked a field of research that has gone on to produce a number of important results regarding the cooperative and often concomitant ordering of these degrees of freedom: just as spins can spontaneously organize into regular arrangements and produce myriad types of magnetism, orbital degrees of freedom can also spontaneously order into regular patterns. Such orbital order has been identified using polarized neutron diffraction to measure its effect on the magnetic form factor in for example K<sub>2</sub>CuF<sub>4</sub> [38], or by measuring how it influences charge distributions in x-ray or electron diffraction in materials like NdSr<sub>2</sub>Mn<sub>2</sub>O<sub>7</sub> [39]. The first direct observation of orbital order, however, was established for LaMnO<sub>3</sub> and La<sub>0.5</sub>Sr<sub>1.5</sub>MnO<sub>4</sub> using resonant x-ray-scattering (RXS) experiments [40,41]. All of these materials are three-dimensional Mott insulators, characterized by strong Coulomb interactions and correspondingly large variations of orbital occupancy.

Here, we use resonant x-ray-scattering measurements at the titanium K edge to reveal the onset of long-range orbital order among the titanium  $d$  orbitals of the weakly coupled van der Waals material  $1T$ -TiSe<sub>2</sub>, within its well-known charge ordered phase. This orbital order does not depend on or conflict with any of the proposed driving mechanisms for the charge density wave. It does mediate a strong interaction with spin, charge, and lattice degrees of freedom and thus

not only represents a new ordered phase of matter for VdW materials, but also offers an inroad for engineering complex phase diagrams and devices with beyond-graphene capability.

## II. ORBITAL ORDER IN TiSe<sub>2</sub>

The quasi-two-dimensional layers of  $1T$ -TiSe<sub>2</sub> consist of titanium atoms in a triangular arrangement, sandwiched between similar planes of selenium atoms and separated from neighboring sandwich layers by a large van der Waals gap, as shown schematically in Fig. 1(a) [42]. The octahedral coordination of selenium atoms around each titanium splits the titanium  $d$  shell into three  $t_{2g}$  and two  $e_g$  orbitals. The subsequent hybridization between low-energy  $t_{2g}$  orbitals and selenium  $p$  orbitals lies at the root of charge and orbital order in TiSe<sub>2</sub> [26].

Cooling down from high temperatures, the uniform, metallic state gives way to a well-known charge ordered (CDW) state at  $T_{\text{CDW}} \simeq 200$  K, with atomic displacements [shown in Fig. 1(b)] known from neutron diffraction experiments [16]. Owing to the lattice symmetry, the charge order in TiSe<sub>2</sub> is a so-called triple- $Q$  charge density wave, consisting of three superposed one-dimensional waves related to one another by 120° rotations. In each of these, symmetry dictates that electronic charge is transferred within a specific set of titanium  $t_{2g}$  and selenium  $p$  orbitals, as indicated in Fig. 1(b) [26]. The atomic displacements in each of the single- $Q$  CDW components can then be understood as the shortening (extension) of Ti-Se bonds with electronic (anti)bonding states. Notice that as long as the threefold rotational symmetry of the lattice remains unbroken, all  $t_{2g}$  orbitals remain equally occupied.

The three components of the charge ordered state are not independent, and influence one another through local Coulomb interactions. On the basis of theoretical considerations it has been proposed that these yield a second phase transition in  $\text{TiSe}_2$ , in which the three CDW components slide by different amounts in order to minimize the real-space overlap of electronic charge [26,27]. This results in a redistribution of charge between different  $t_{2g}$  orbitals, and thus an orbital ordered (OO) state that breaks both the threefold rotational and inversion symmetries of the high-temperature phases. The atomic displacements associated with the shifting CDW components reflect the broken symmetries, and are expected to yield the low-temperature configuration shown in Fig. 1(c). However, the changes in atomic displacement upon entering the OO phase may be expected to be exceedingly small, and evade detection in scanning-tunneling microscopy (STM) and x-ray-diffraction experiments [16,29], complicating experimental verification of this proposed mechanism. The sliding of CDW components by different amounts under the influence of Coulomb interactions and causing spatial modulations in the occupation of orbitals is believed to be generic for multicomponent CDW materials, and has been suggested to be at play in the same form in other TMDC compounds, such as  $2H\text{-TaS}_2$ , as well as some elemental materials, like Se, Te, and Po [26,34,43,44].

The actual presence of broken inversion symmetry associated with orbital order in  $\text{TiSe}_2$  has been the subject of intense debate [29–31]. On the one hand, there is indirect evidence of a phase transition at temperatures slightly below  $T_{\text{CDW}}$  [27], and STM experiments reporting the formation of domains that appear to have different senses of handedness [45]. These are contested however by other groups who observe no evidence of broken inversion symmetry in STM or other probes [29]. The paradox is further fueled by lack of any direct impact of the breakdown of inversion on scattering experiments, and the practical complication of bulk probes necessarily averaging over many domains of different handedness, thus precluding any direct measurement of broken inversion symmetry. Recently, photogalvanic effect measurements were able to conclusively show inversion symmetry to be broken in the low-temperature phase of samples cooled through their ordering transition in the presence of a strong circularly polarized light field [46]. Because of the active training, however, these results do not rule out the possibility that untrained samples of  $\text{TiSe}_2$  remain inversion symmetric.

Here, we find that orbital order, rather than the breakdown of inversion symmetry, is actually the main characteristic of the low-temperature phase of  $\text{TiSe}_2$ . The RXS experiments presented here, supported by first-principles calculations, show direct experimental evidence for the presence of an orbital ordered phase in  $\text{TiSe}_2$ . Crucially, because the observed signal is sensitive to uneven orbital occupation rather than handedness or broken inversion symmetry, it is not necessary to train the sample with an applied field, allowing us to detect symmetry breaking that is truly spontaneous.

### III. X-RAY SCATTERING

Although RXS at the main K edge corresponds to the  $1s \rightarrow 4p$  transition, orbital order in  $3d$  transition-metal

compounds can nonetheless be probed at its pre-edge [47,48]. This is made possible by three complementary processes, all of which may be expected to contribute to the signal in  $\text{TiSe}_2$  to some extent. First of all, Ti  $3d$  orbitals contribute to the pre-edge of this transition their hybridization with ligand Se  $4p$  orbitals that are in turn hybridized with  $4p$  orbitals of neighboring Ti atoms. This mechanism is driven by the covalent nature of  $\text{TiSe}_2$  and does not require the breakdown of inversion symmetry. If inversion is broken, however, some direct hybridization between Ti  $3d$  and  $4p$  orbitals at the same site may occur and give rise to additional intensity at the pre-edge. Finally, direct quadrupole-quadrupole transitions at the superlattice peak positions become allowed whenever there is an uneven occupation of the Ti  $3d$  orbitals.

Hence, we performed RXS measurements at the Ti K edge to investigate the ordering of Ti  $3d$  orbitals of  $t_{2g}$  symmetry (see Methods section for sample preparation and experimental setup). In agreement with RXS measurements at the Se K edge [49], the observed CDW reflections may be divided into qualitatively different groups, based on their energy dependence. Unlike the Se-based measurements, however, we find that the different energy profiles of the Ti K edge reflections allow us to assign them to distinct scattering processes and yield direct evidence for the presence of orbital order.

The first group of reflections contains conventional CDW peaks, like the  $(0.5, 0.5, 0.5)$  reflection shown in Fig. 2(a), which are also visible in nonresonant scattering experiments. Their energy line shape is similar to that of the primary Bragg peaks, included for comparison in Fig. 2(c). These signals are dominated by Thomson scattering from atomic cores, and give a direct measure of the lattice displacements in the CDW phase. Since all electrons on the Ti atoms participate in this type of scattering process, it yields a large overall intensity. It does not have a strong energy dependence, except for a sharp suppression near the resonant edge, that follow the normal dispersion of the Ti atomic scattering factor near this edge. Figure 2(e) shows the integrated intensity of the peak in panel (a). Fitting with a universal power-law function (see Methods section for details) yields an estimated transition temperature of  $T_{\text{CDW}} \approx 193$  K, which is consistent with resistivity measurements on a sample from the same batch.

Intriguingly, we identified a second group of RXS signals at points in  $k$  space where reflections are absent in nonresonant experiments, such as  $(0.5, 0, 0.5)$  shown in Fig. 2(b) [another example,  $(2.5, 0, 0.5)$ , is shown in the Supplemental Material [50]]. It should be noted that the apparent broader width of the  $(0.5, 0, 0.5)$  peak arises from the multigrain structure of the measured sample and does not indicate a difference in correlation length. The structure factor at these momenta is strictly zero as long as the crystal structure of  $\text{TiSe}_2$  is either  $P\bar{3}m1$  or  $P\bar{3}c1$ , corresponding to the symmetries of the high-temperature phase and the CDW state without orbital order, respectively [16] (see Supplemental Material [50] for details of the calculation). The origin for the reflections in the present experiment can be clarified from their energy dependence. Unlike what would be expected from Thomson scattering, these signals have a strong, resonant peak at the pre-edge of the Ti K edge, as shown in Fig. 2(d). This is typical for reflections originating in transitions between specific orbital states, involving only a few electrons that can be efficiently

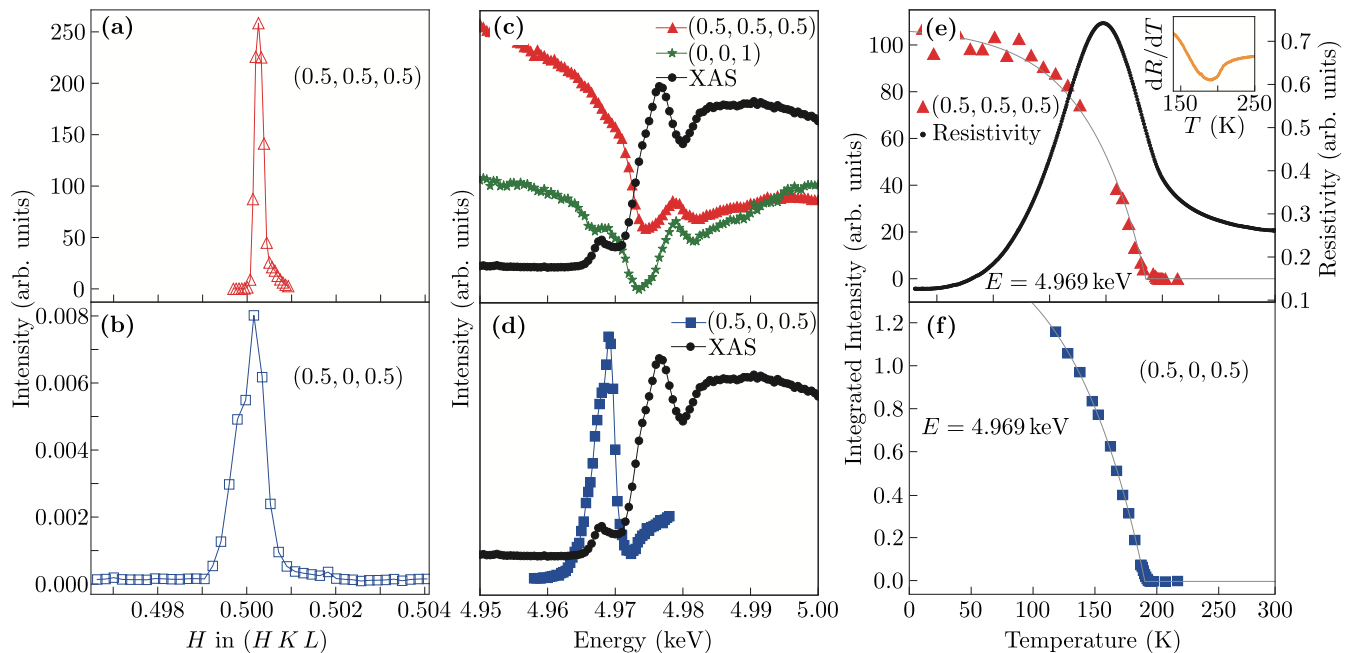


FIG. 2. Charge density wave and orbital order in  $\text{TiSe}_2$  and their energy and temperature dependence measured by RXS at the Ti K edge. (a, b) H cuts at 11 K for  $(0.5, 0.5, 0.5)$  and  $(0.5, 0, 0.5)$ , respectively. (c, d) Corresponding energy scans near the Ti K edge. The x-ray-absorption spectrum (XAS) at the Ti K edge is shown for comparison, as is the energy scan for the  $(0, 0, 1)$  Bragg peak. (e, f) Temperature dependence at 4.969 keV of the peaks at  $(0.5, 0.5, 0.5)$  and  $(0.5, 0, 0.5)$ , respectively. The resistivity measurement is displayed in (e) for comparison, with the inset showing its derivative close to the transition temperature. The gray solid lines are fits to the data showing a transition temperature  $T_{\text{cdw}} \approx 193$  K.

excited only near resonance [51]. For this type of reflection, the local density of states dominates the energy dependence of the scattering intensity.

The presence of a second group of reflections, originating from transitions between specific orbital states, implies that titanium atoms with the same number of electrons, the structure factors of which cancel in Thomson scattering, must have inequivalent orbital structures that allow these reflections under resonant conditions. In other words, the orbital occupations of the titanium atoms follow a regular pattern with lower symmetry than the high-temperature state and conventional CDW phase. The observation of peaks like  $(0.5, 0, 0.5)$  and  $(2.5, 0, 0.5)$ , with energy dependencies dominated by orbital-specific transitions, thus constitutes direct evidence of orbital order in the low-temperature phase of  $\text{TiSe}_2$ . Based on fits of the thermal evolutions of integrated intensities for these new reflections, shown in Fig. 2(f), we find the onset temperature of the novel orbital ordered state and the conventional CDW phase to be indistinguishable within the experimental resolution.

Although the orbital order is primarily manifested in the occupation of titanium  $t_{2g}$  orbitals, it also has an effect on atomic displacements. This is evidenced in yet a third class of reflections that we observe, the energy dependence of which indicates interference between conventional Thomson scattering and resonant orbital scattering channels [for example, the peak  $(0.5, 0.5, 2.5)$  is shown in the Supplemental Material [50]]. These reflections are significantly enhanced compared to nonresonant experiments near the Ti K edge, but also show the largely energy-independent background characteristic of

atomic scattering. The enhancement of these reflections can be viewed as a secondary effect of the onset of orbital order, and showcase the strong coupling between orbital, lattice, and charge degrees of freedom.

It should be noted that our results are complementary to earlier experiments on the Se K edge [49], in which similar sets of nonresonantly forbidden reflections were identified. The nonzero intensity in these experiments was attributed to anisotropic tensor susceptibility (ATS) or Templeton-Templeton scattering [52,53]. The presence of this type of scattering indicates that the electronic density on Se sites is aspherical, and thus an unequal local population of Se  $p$  orbitals. Indeed, such unequal occupation is expected in all proposed charge ordered phases of  $\text{TiSe}_2$ , both with and without inversion symmetry. It does not constitute orbital order of the strongly delocalized ligand Se  $p$  states, however, in much the same way that oxygen  $p$  orbitals in  $\text{LaMnO}_3$  or  $\text{La}_{0.5}\text{Sr}_{1.5}\text{MnO}_4$  are not considered to be orbitally ordered. Instead, true orbital order is expected to emerge among the localized  $d$  states of the transition-metal atoms, such as the Ti  $t_{2g}$  states investigated here.

All three mechanisms that may contribute to the presently observed intensity at the pre-edge imply the presence of order among the Ti  $d$  orbitals. For some this would arise as a direct consequence of broken inversion symmetry (mixing with Ti  $4p$  orbitals) while for others it is an indirect effect of the lattice distortions associated with any type of charge order in  $\text{TiSe}_2$  (broken rotational symmetry due to uneven mixing with ligand Se  $p$  orbitals caused by lattice distortions). Although the former is a more direct effect, we cannot conclusively

determine which channel dominates our observations. Regardless of the driving mechanism, however, our results firmly establish the presence of orbital order among the Ti  $t_{2g}$  states. This goes beyond the expected ATS scattering at Se sites, and allows a direct comparison to strongly coupled orbital ordered oxides.

#### IV. FIRST-PRINCIPLES RESULTS

A possible way for orbital order to emerge in  $\text{TiSe}_2$  is suggested by a Ginzburg-Landau theory predicting that different CDW components obtain phase shifts relative to one another [26]. Adding corresponding phase shifts to the atomic displacements gives a model for the corresponding atomic configuration of the OO phase (see Supplemental Material [50] for details). To obtain microscopic insight into the effects of orbital order, we consider structures with different phase shifts and calculate projected density of states (PDOS) by means of density functional theory (DFT) calculations. As resonant peaks are underlain by uneven orbital occupations [54–57], the RXS structure factor is proportional to a linear combination of the PDOS for all Ti atoms in the unit cell. In Fig. 3(a), we demonstrate that a particular linear combination of Ti- $4p$  orbitals reflecting the expected difference in orbital occupation between consecutive layers yields a nonzero scattering amplitude in structures with nonzero relative phase shifts.

As shown schematically in Fig. 3(b), the onset of this signal implies differences between the densities of symmetry-related orbitals at fixed energy, and indicates a breakdown of both inversion and threefold rotational symmetries. The presence of orbital order thus allows for resonant reflections that are forbidden in the CDW structure without relative phase shifts. Notice that because  $\text{TiSe}_2$  is a weakly coupled material, the absolute variations in orbital occupation may be expected to be much lower than those in strongly correlated insulators, such as the archetypical orbitally ordered material  $\text{LaMnO}_3$  [40]. Nevertheless, a systematic investigation of which forbidden peaks become allowed and gain significant amplitude in the OO phase (see Supplemental Material [50]) shows that both the momenta at which such reflections emerge, and the energy dependence of the predicted signal, are consistent with the RXS experiments.

#### V. CONCLUSIONS

We report experimental evidence for the existence of orbital order in the low-temperature phase of  $1T$ - $\text{TiSe}_2$ , consistent with first-principles predictions based on a theoretical model for combined charge and orbital order, and independent of the driving mechanism behind the charge density wave formation.

These observations pave the way for exploring orbital order in other low-dimensional, weakly coupled materials. Based on the general nature of the mechanism stabilizing the OO phase, one expects very similar types of orbital order to be common in determining physical properties throughout TMDC with commensurate multicomponent charge order, like  $2H$ - $\text{TaS}_2$  or  $1T$ - $\text{VSe}_2$ , but also more generally in beyond-graphene van der Waals materials.

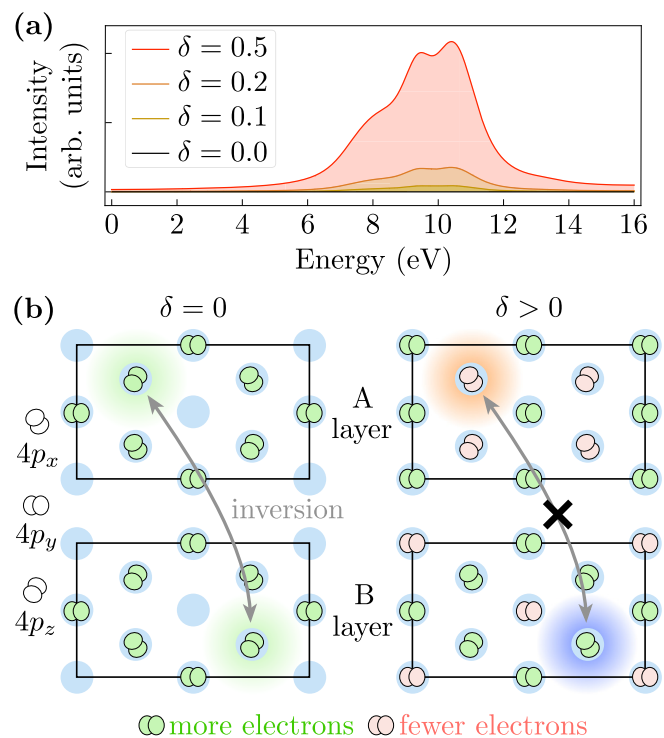


FIG. 3. Energy dependence of the scattering amplitude in the orbital ordered phase. (a) Expected energy dependence of the scattering amplitude, with its characteristic resonance structure, based on the square of the orbital-resolved projected densities of states (see Supplemental Material [50]), and broadened to reflect the effect of finite lifetimes. Different curves represent different values of the relative phase shift between CDW components. The energy scale on the horizontal axis is measured with respect to the Fermi level. (b) Ti  $4p$  orbital densities at fixed energy in the atomic structures with zero (left) and nonzero (right) relative phase shift  $\delta$  between CDW components. For  $\delta = 0$ , three out of four Ti sites have one predominant  $4p$  orbital (green), while orbitals with lower density are degenerate. The structures in neighboring planes are related by inversion. For nonzero relative phase shift, the densities of some previously degenerate orbitals increase (green) or decrease (red). The pattern of orbital polarization shown here for Ti  $4p$  orbitals is also present in the densities of other orbitals, and breaks both inversion and threefold rotational symmetry.

As all charge transfer processes take place within individual  $\text{TiSe}_2$  sandwiches, the orbital order is expected to survive even in the monolayer limit. This, together with the strong interplay between orbital occupation and charge, lattice, and spin degrees of freedom, gives great potential to the orbital order as a promising route to tuning and manipulating the physical responses in devices based on van der Waals materials.

#### VI. METHODS

##### A. Sample preparation

We synthesized  $1T$ - $\text{TiSe}_2$  single crystals in two steps. First, polycrystalline  $1T$ - $\text{TiSe}_2$  powders were synthesized in solid state, by grinding stoichiometric quantities of the reactants of Ti (Alfa Aesar, 99.9%) and Se (Alfa Aesar, 99.999%) in

an agate mortar. The mixture was then transferred to a quartz tube and sealed under high vacuum. Polycrystalline samples were obtained after heating at 550 °C for 120 h. Second, single crystals of 1T-TiSe<sub>2</sub> were grown using the chemical vapor transport method, with I<sub>2</sub> as the transport agent. The as-prepared polycrystalline 1T-TiSe<sub>2</sub> powders were mixed with I<sub>2</sub> in a quality ratio of about 20:1. The mixtures sealed in vacuum quartz tubes were then heated for seven days in a two-zone furnace, where the source and growth zone temperatures were 700 and 600 °C, respectively. Resistivity measurements using the four-points method were performed on single crystals taken from the same batch of samples as that used for RXS experiments.

### B. RXS measurements

The RXS experiments were performed at beam line 4-ID-D of the Advanced Photon Source at Argonne National Laboratory. The TiSe<sub>2</sub> crystal was mounted on an aluminum sample holder and cooled with a closed-cycle cryostat attached to a four-circle diffractometer. Experiments were done by integrating over all scattered photon energies. The linear polarization was collected with  $\sigma$ -incident polarization (perpendicular to the scattering plane). The x-ray-absorption spectrum was obtained by integrating the fluorescence signal. The observed pre-edge feature in these spectra is well known to be related to the *d* electrons [51]. The temperature dependence of  $T_{\text{CDW}}$  can be well fitted using the empirical function  $f(t) = t_0\{1 - [(t + \alpha)/(1 + \alpha)]^\beta\}$ , with  $t = T/T_{\text{CDW}}$  the reduced temperature, and  $\alpha$ ,  $\beta$ , and  $T_{\text{CDW}}$  used as fitting parameters [58].

### C. First-principles prediction of RXS intensities

We perform density functional theory band-structure calculations using the generalized gradient approximation [59], as implemented in the full-potential code FPLO version 18 [60].

Although the structures without relative phase shifts feature a higher symmetry than those with phase shifts, we perform all calculations within the same low-symmetry monoclinic space group *C*2 to ensure that all structures are treated on equal footing. Within each phase, we impose the crystal symmetries of the respective structural input and preclude structural relaxations so that the type of symmetry-allowed order present in each DFT calculation is determined by the structural input. The low symmetry of the unit cell gives rise to numerical noise in the calculated projected DOS, which we remedy by using a densely sampled *k* mesh of  $41 \times 41 \times 24$  points (20 213 points in the irreducible wedge).

### ACKNOWLEDGMENTS

Y.Y.P. is grateful for financial support from the National Natural Science Foundation of China (Grant No. 11974029). P.A. acknowledges support from the Gordon and Betty Moore Foundation, Grant No. GMBF-9452. RXS experiments were supported by the U.S. Department of Energy Grant No. DE-FG02-06ER46285, with use of the Advanced Photon Source supported by DOE Contract No. DE-AC02-06CH11357. H.X.L. acknowledges financial support from the National Natural Science Foundation of China (Grant No. 11922415). J.v.d.B acknowledges the Deutsche Forschungsgemeinschaft for support through the Würzburg-DresdenCluster of Excellence on Complexity and Topology in Quantum Matter ct.qmat (EXC 2147, Project No. 39085490) and the Collaborative Research Center SFB 1143 (Project No. 247310070).

J.v.d.B., P.A., Y.Y.P., and J.v.W. conceived and designed the experiments and calculations; Y.Y.P. and X.F.G. performed the RXS experiment at Advanced Photon Source with the help of J.S. and Y.C. H.X.L. and D.Y. grew the TiSe<sub>2</sub> samples; S.J. and Y.Q.H. performed the resistivity measurement; Y.Y.P., Q.X., Q.Z.L., and X.F.G. analyzed the experimental data; J.v.W. modeled atomic displacements and O.J. performed the first-principles calculations; J.v.W. wrote the paper with input from all authors.

- 
- [1] M. M. Otrokov, I. I. Klimovskikh, H. Bentmann, D. Estyunin, A. Zeugner, Z. S. Aliev, S. Gaß, A. U. B. Wolter, A. V. Koroleva, A. M. Shikin *et al.*, Prediction and observation of an antiferromagnetic topological insulator, *Nature (London)* **576**, 416 (2019).
- [2] T. Li, S. Jiang, N. Sivadas, Z. Wang, Y. Xu, D. Weber, J. E. Goldberger, K. Watanabe, T. Taniguchi, C. J. Fennie *et al.*, Pressure-controlled interlayer magnetism in atomically thin CrI<sub>3</sub>, *Nat. Mater.* **18**, 1303 (2021).
- [3] W. Chen, Z. Sun, Z. Wang, L. Gu, X. Xu, S. We, and C. Gao, Direct observation of van der Waals stacking-dependent interlayer magnetism, *Science* **366**, 983 (2019).
- [4] D. MacNeill, J. T. Hou, D. R. Klein, P. Zhang, P. Jarillo-Herrero, and L. Liu, Gigahertz Frequency Antiferromagnetic Resonance and Strong Magnon-Magnon Coupling in the Layered Crystal CrCl<sub>3</sub>, *Phys. Rev. Lett.* **123**, 047204 (2019).
- [5] C. Gong, E. M. Kim, Y. Wang, G. Lee, and X. Zhang, Multiferroicity in atomic van der Waals heterostructures, *Nat. Commun.* **10**, 2657 (2019).
- [6] S. Kang, K. Kim, B. H. Kim, J. Kim, K. Ik Sim, J.-U. Lee, S. Lee, K. Park, S. Yun, T. Kim *et al.*, Coherent many-body exciton in van der Waals antiferromagnet NiPS<sub>3</sub>, *Nature* **583**, 785 (2020).
- [7] Y. Wu, S. Zhang, J. Zhang, W. Wang, Y. L. Zhu, J. Hu, G. Yin, K. Wong, C. Fang, C. Wan *et al.*, Néel-type skyrmion in WTe<sub>2</sub>/Fe<sub>3</sub>GeTe<sub>2</sub> van der Waals heterostructure, *Nat. Commun.* **11**, 3860 (2020).
- [8] A. Devarakonda, H. Inoue, S. Fang, C. Ozsoy-Keskinbora, T. Suzuki, M. Kriener, L. Fu, E. Kaxiras, D. C. Bell, and J. G. Checkelsky, Clean 2D superconductivity in a bulk van der Waals superlattice, *Science* **371**, 231 (2020).
- [9] R. Noguchi, M. Kobayashi, Z. Jiang, K. Kuroda, T. Takahashi, Z. Xu, D. Lee, M. Hirayama, M. Ochi, T. Shirasawa *et al.*, Evidence for a higher-order topological insulator in a three-dimensional material built from van der Waals stacking of bismuth-halide chains, *Nat. Mater.* **20**, 473 (2021).
- [10] J. Diego, A. H. Said, S. K. Mahatha, Raffaello Bianco, Lorenzo Monacelli, Matteo Calandra, Francesco Mauri, K. Rossnagel,

- Ion Errea, and S. Blanco-Canosa, Van der Waals driven anharmonic melting of the 3D charge density wave in  $\text{VSe}_2$ , *Nat. Commun.* **12**, 598 (2021).
- [11] A. K. Geim and I. V. Grigorieva, Van der waals heterostructures, *Nature (London)* **499**, 419 (2013).
- [12] K. S. Novoselov, A. Mishchenko, A. Carvalho, and A. H. Castro Neto, 2D materials and van der Waals heterostructures, *Science* **353**, aac9439 (2016).
- [13] A. F. Kusmartseva, B. Sipos, H. Berger, L. Forró, and E. Tutiš, Pressure Induced Superconductivity in Pristine 1T-TiSe<sub>2</sub>, *Phys. Rev. Lett.* **103**, 236401 (2009).
- [14] E. Morosan, H. W. Zandbergen, B. S. Dennis, J. W. G. Bos, Y. Onose, T. Klimczuk, A. P. Ramirez, N. P. Ong, and R. J. Cava, Superconductivity in  $\text{Cu}_x\text{TiSe}_2$ , *Nat. Phys.* **2**, 544 (2006).
- [15] L. J. Li, E. C. T. O'Farrell, K. P. Loh, G. Eda, B. Özyilmaz, and A. H. Castro Neto, Controlling many-body states by the electric-field effect in a two-dimensional material, *Nature (London)* **529**, 185 (2016).
- [16] F. J. Di Salvo, D. E. Moncton, and J. V. Waszczak, Electronic properties and superlattice formation in the semimetal  $\text{TiSe}_2$ , *Phys. Rev. B* **14**, 4321 (1976).
- [17] K. Rossnagel, L. Kipp, and M. Skibowski, Charge-density-wave phase transition in 1T-TiSe<sub>2</sub>: Excitonic insulator versus band-type Jahn-Teller mechanism, *Phys. Rev. B* **65**, 235101 (2002).
- [18] J. A. Wilson, Concerning the semimetallic characters of  $\text{TiS}_2$  and  $\text{TiSe}_2$ , *Solid State Commun.* **22**, 551 (1977).
- [19] H. Cercellier, C. Monney, F. Clerc, C. Battaglia, L. Despont, M. G. Garnier, H. Beck, P. Aebi, L. Patthey, H. Berger, and L. Forró, Evidence for an excitonic insulator phase in 1T-TiSe<sub>2</sub>, *Phys. Rev. Lett.* **99**, 146403 (2007).
- [20] H. P. Hughes, Structural distortion in  $\text{TiSe}_2$  and related materials - a possible Jahn-Teller effect? *J. Phys. C* **10**, L319 (1977).
- [21] N. Suzuki, A. Yamamoto, and K. Motizuki, Microscopic theory of the cdw state of 1T-TiSe<sub>2</sub>, *J. Phys. Soc. Jpn.* **54**, 4668 (1985).
- [22] T. E. Kidd, T. Miller, M. Y. Chou, and T.-C. Chiang, Electron-Hole Coupling and the Charge Density Wave Transition in  $\text{TiSe}_2$ , *Phys. Rev. Lett.* **88**, 226402 (2002).
- [23] M. Calandra and F. Mauri, Charge-Density Wave and Superconducting Dome in  $\text{TiSe}_2$  from Electron-Phonon Interaction, *Phys. Rev. Lett.* **106**, 196406 (2011).
- [24] A. Kogar, M. S. Rak, S. Vig, A. A. Husain, F. Flicker, Y. I. Joe, L. Venema, G. J. MacDougall, T. C. Chiang, E. Fradkin *et al.*, Signatures of exciton condensation in a transition metal dichalcogenide, *Science* **358**, 1314 (2017).
- [25] J. van Wezel, P. Nahai-Williamson, and S. S. Saxena, Exciton-phonon-driven charge density wave in  $\text{TiSe}_2$ , *Phys. Rev. B* **81**, 165109 (2010).
- [26] J. van Wezel, Chirality and orbital order in charge density waves, *Europhys. Lett.* **96**, 67011 (2011).
- [27] J.-P. Castellán, S. Rosenkranz, R. Osborn, Q. Li, K. E. Gray, X. Luo, U. Welp, G. Karapetrov, J. P. C. Ruff, and J. van Wezel, Chiral Phase Transition in Charge Ordered 1T-TiSe<sub>2</sub> *Phys. Rev. Lett.* **110**, 196404 (2013).
- [28] M. Gradhand and J. van Wezel, Optical gyrotropy and the nonlocal Hall effect in chiral charge-ordered  $\text{TiSe}_2$ , *Phys. Rev. B* **92**, 041111(R) (2015).
- [29] B. Hildebrand, T. Jaouen, M.-L. Mottas, G. Monney, C. Barreateau, E. Giannini, D. R. Bowler, and P. Aebi, Local real-space view of the achiral 1T-TiSe<sub>2</sub>  $2 \times 2 \times 2$  charge density wave, *Phys. Rev. Lett.* **120**, 136404 (2018).
- [30] M.-K. Lin, J. A. Hlevyack, P. Chen, R.-Y. Liu and T.-C. Chiang, Comment on “Chiral Phase Transition in Charge Ordered 1T-TiSe<sub>2</sub>”, *Phys. Rev. Lett.* **122**, 229701 (2019).
- [31] S. Rosenkranz, R. Osborn, and J. van Wezel, Rosenkranz, Osborn, and Van Wezel Reply, *Phys. Rev. Lett.* **122**, 229702 (2019).
- [32] Y. Tokura, and N. Nagaosa, Orbital physics in transition-metal oxides, *Science* **288**, 462 (2000).
- [33] T. Ritschel, J. Trinckauf, K. Koepf, B. Bchner, M. v. Zimmermann, H. Berger, Y. I. Joe, P. Abbamonte, and J. Geck, Orbital textures and charge density waves in transition metal dichalcogenides, *Nat. Phys.* **11**, 328 (2015).
- [34] A. Silva and J. van Wezel, The simple-cubic structure of elemental polonium and its relation to combined charge and orbital order in other elemental chalcogens, *SciPost Phys.* **4**, 028 (2018).
- [35] F. Flicker and J. van Wezel, Charge order in  $\text{NbSe}_2$ , *Phys. Rev. B* **94**, 235135 (2016).
- [36] K. I. Kugel and D. I. Khomskii, Crystal-structure and magnetic properties of substances with orbital degeneracy, *Zh. Eksp. Teor. Fiz* **64**, 1429 (1973) [*Sov. Phys. JETP* **37**, 725 (1973)].
- [37] K. I. Kugel and D. I. Khomskii, The Jahn-Teller effect and magnetism: Transition metal compounds, *Sov. Phys. Usp.* **25**, 231 (1982).
- [38] F. Moussa and J. Villain, Spin-wave lineshape in two-dimensional  $\text{K}_2\text{CuF}_4$ : Neutron experiments and theory, *J. Phys. C* **9**, 4433 (1976).
- [39] M. Takata, E. Nishibori, K. Kato, M. Sakata, and Y. Morimoto, Direct observation of orbital order in manganites by mem charge-density study, *J. Phys. Soc. Jpn.* **68**, 2190 (1999).
- [40] Y. Murakami, J. P. Hill, D. Gibbs, M. Blume, I. Koyama, M. Tanaka, H. Kawata, T. Arima, Y. Tokura, K. Hirota, and Y. Endoh, Resonant X-Ray Scattering from Orbital Ordering in  $\text{LaMnO}_3$ , *Phys. Rev. Lett.* **81**, 582 (1998).
- [41] U. Staub, V. Scagnoli, A. M. Mulders, M. Janousch, Z. Honda, and J. M. Tonnerre, Charge/orbital ordering vs. Jahn-Teller distortion in  $\text{La}_{0.5}\text{Sr}_{1.5}\text{MnO}_4$ , *Europhys. Lett.* **76**, 926 (2006).
- [42] M. H. Whangbo and E. Canadell, Analogies between the concepts of molecular chemistry and solid-state physics concerning structural instabilities. electronic origin of the structural modulations in layered transition metal dichalcogenides, *J. Am. Chem. Soc.* **114**, 9587 (1992).
- [43] J. van Wezel, Polar charge and orbital order in  $2H\text{-TaS}_2$ , *Phys. Rev. B* **85**, 035131 (2012).
- [44] A. Silva, J. Henke, and J. van Wezel, Elemental chalcogens as a minimal model for combined charge and orbital order, *Phys. Rev. B* **97**, 045151 (2018).
- [45] M. Iavarone, R. DiCapua, X. Zhang, M. Golalikhani, S. A. Moore, and G. Karapetrov, Evolution of the charge density wave state in  $\text{Cu}_x\text{TiSe}_2$ , *Phys. Rev. B* **85**, 155103 (2012).
- [46] S.-Y. Xu, Q. Ma, Y. Gao, A. Kogar, A. Zong, A. M. Mier Valdivia, T. H. Dinh, S.-M. Huang, B. Singh, C.-H. Hsu *et al.*, Spontaneous gyrotropic electronic order in a transition-metal dichalcogenide, *Nature (London)* **578**, 545 (2020).
- [47] R. Vedrinskii, V. Kraizman, A. Novakovich, P. V. Demekhin, and S. Urazhdin, Pre-edge fine structure of the 3d atom K x-ray absorption spectra and quantitative atomic structure determi-

- nations for ferroelectric perovskite structure crystals, *J. Phys.: Condens. Matter* **10**, 9561 (1998).
- [48] F. De Groot, G. Vankó, and P. Glatzel, The 1s x-ray absorption pre-edge structures in transition metal oxides, *J. Phys.: Condens. Matter* **21**, 104207 (2009).
- [49] H. Ueda, M. Porer, J. R. L. Mardegan, S. Parchenko, N. Gurung, F. Fabrizi, M. Ramakrishnan, L. Boie, M. Josef Neugebauer, B. Burganov *et al.*, Correlation between electronic and structural orders in 1T-TiSe<sub>2</sub>, *Phys. Rev. Research* **3**, L022003 (2021).
- [50] See Supplemental Material at <http://link.aps.org/supplemental/10.1103/PhysRevResearch.4.033053> for details of RXS reflections and dichroism experiments not discussed in the main text, as well as the calculated structure factors for reflections that are forbidden in any configuration with simultaneous inversion and three-fold rotational symmetries.
- [51] T. Yamamoto, Assignment of pre-edge peaks in k-edge x-ray absorption spectra of 3d transition metal compounds: Electric dipole or quadrupole? *X-Ray Spectrom.* **37**, 572 (2008).
- [52] D. Templeton and L. Templeton, X-ray dichroism and polarized anomalous scattering of the uranyl ion, *Acta Cryst. A* **38**, 62 (1982).
- [53] V. E. Dmitrienko, Forbidden reflections due to anisotropic x-ray susceptibility of crystals, *Acta Cryst. A* **39**, 29 (1983).
- [54] I. S. Elfimov, V. I. Anisimov, and G. A. Sawatzky, Orbital Ordering, Jahn-Teller Distortion, and Anomalous X-Ray Scattering in Manganates, *Phys. Rev. Lett.* **82**, 4264 (1999).
- [55] M. Takahashi, J.-i. Igarashi, and P. Fulde, Anomalous x-ray scattering in LaMnO<sub>3</sub>, *J. Phys. Soc. Jpn.* **68**, 2530 (1999).
- [56] P. Mahadevan, K. Terakura, and D. D. Sarma, Spin, Charge, and Orbital Ordering in La<sub>0.5</sub>Sr<sub>1.5</sub>MnO<sub>4</sub>, *Phys. Rev. Lett.* **87**, 066404 (2001).
- [57] P. Benedetti, J. van den Brink, E. Pavarini, A. Vigliante, and P. Wochner, *Ab initio* calculation of resonant X-ray scattering in manganites, *Phys. Rev. B* **63**, 060408(R) (2001).
- [58] Y. I. Joe, X. M. Chen, P. Ghaemi, K. D. Finkelstein, G. A. de la Peña, Y. Gan, J. C. T. Lee, S. Yuan, J. Geck, G. J. MacDougall, T. C. Chiang *et al.*, Emergence of charge density wave domain walls above the superconducting dome in 1T-TiSe<sub>2</sub>, *Nat. Phys.* **10**, 421 (2014).
- [59] J. P. Perdew, K. Burke, and M. Ernzerhof, Generalized Gradient Approximation Made Simple, *Phys. Rev. Lett.* **77**, 3865 (1996).
- [60] K. Koepnick, and H. Eschrig, Full-potential nonorthogonal local-orbital minimum-basis band-structure scheme, *Phys. Rev. B* **59**, 1743 (1999).